JOURNAL OF AIRCRAFT
Vol. 39, No. 6, November–December 2002

Extension of Wake-Survey Analysis Method to Cover Compressible Flows

Kazuhiro Kusunose* and James P. Crowder†
The Boeing Company, Seattle, Washington 98124-2207

This paper summarizes the work accomplished over the last several years on wake-survey analysis method developments at Boeing. In this paper Betz and Maskell's lift-and-drag equations are extended to cover compressible flows. The small perturbation method is employed to expand the general lift-and-drag equations in the momentum integral forms, assuming downstream states that differ only slightly from the state of approach. Introducing new, simpler, and cleaner expansion procedures, it is proven that both the lift and drag of an airplane model can be predicted accurately by simply measuring flow variables inside of the model wake region. This result enables the practical application of quantitative wake surveys for accurate lift-and-drag predictions of airplane models. To demonstrate the current lift-and-drag prediction capabilities, some wake-survey analysis results from previously published data are recalculated. Because wake surveys are not needed outside of the model wake region, one complete wake survey analysis for a nonpowered engine case, including data acquisitions and reductions, can now be finished in approximately 10–15 min. These wake-survey analysis results demonstrate that both wake-integrated lift and drag typically agree with the internal strain-gauge balance to within a few percentage points.

Nomenclature

a, a_∞	=	local and freestream speeds of sound
b	=	model wing span
C	=	local wing chord
C_D, C_L	=	drag and lift coefficients
C_d, C_l	=	wing section drag and lift coefficients
C_p, C_v	=	specific heats
D	=	drag
D_{ct}	=	drag correction term
D_e	=	enthalpy drag
D_{jet}	=	drag calculated from jet wake regions
D_{Mi}	=	Maskell's induced drag
D_m	=	injected mass drag (thrust)
D_p	=	profile drag
D_{reg}	=	drag calculated from regular wake regions
$\boldsymbol{F}$	=	force acting on an airplane model
h, h_∞, Δh	=	local, freestream, and perturbation enthalpies
h_T, h_{T_∞}	=	local and freestream total enthalpies
$\boldsymbol{I}_x$, $\boldsymbol{I}_y$, $\boldsymbol{I}_z$	=	uint vectors pointing in x, y, and z directions
K	=	small perturbation quantity defined in Eq. (21)
L	=	lift
M, M_∞	=	local and freestream Mach numbers
$\dot{m}$	=	rate of mass injected into the system by powered engines
$\boldsymbol{n}$	=	surface outward unit normal vector (n_x, n_y, n_z)
P, P_∞, ΔP	=	local, freestream, and perturbation pressures
P_T, P_{T_∞}	=	local and freestream total pressures
R	=	gas constant
S	=	control volume surface area
S_F	=	y component of body force
S_2	=	integral area on the entire wake survey plane
s, s_∞, Δs	=	local, freestream, and perturbation entropies
T, T_∞	=	local and freestream temperatures
T_T, T_{T_∞}	=	local and freestream total temperatures
U_∞, Δu	=	local and perturbation velocities in x direction
u, v, w	=	velocity components in x, y, and z directions
$\boldsymbol{u}$	=	velocity vector (u, v, w)
u^*	=	Betz's artificial velocity (Ref. 1)
W_A	=	integral area over the model wake region
$W_{A\,\text{jet}}$	=	integral area over jet wake regions
x, y, z	=	coordinates in freestream, spanwise, and transverse directions
x_{ws}	=	x coordinate of wake survey station
γ	=	ratio of specific heats, C_p/C_v
ΔH	=	change in total enthalpy as a result of the work done by engines
ξ	=	x component of vorticity vector, $\boldsymbol{\omega}$
ρ, ρ_∞, $\Delta\rho$	=	local, freestream, and perturbation densities
σ	=	velocity gradient, $-\partial u/\partial x$
$\boldsymbol{\tau}$	=	viscous and turbulence stress tensor
ϕ, ψ	=	Maskell's scalar functions
$\boldsymbol{\omega}$	=	vorticity vector, $\nabla \times \boldsymbol{u}$

Received 10 December 2001; revision received 11 June 2002; accepted for publication 11 July 2002.

*Research Engineer, Acoustics and Fluid Mechanics, P.O. Box 3707, MS 67-LF; kazuhiro.kusunose@boeing.com. Member AIAA.

†Senior Technical Fellow, Aerodynamics Laboratory, P.O. Box 3707, MS 1W-82; james.p.crowder@boeing.com. Member AIAA.

Introduction

THE forces acting upon a model can generally be derived by applying the integral form of the momentum equations to a control volume containing the model (see Fig. 1). Model lift and drag can be written as integrals of the flow variables measured at a downstream survey station (Fig. 2). The problem with such momentum integral forms is that the integral must be evaluated over the entire downstream cross section at the wake survey station.

Ever since Betz and Maskell[1,2] demonstrated that an integral formulation for forces acting on the model can be obtained from flow variables measured within the model wake region, the practical application of quantitative wake surveys has been feasible.[3–7] To meet the continued need for increasingly accurate lift-and-drag predictions, more refined formulas have constantly been developed. Highly accurate lift-and-drag predictions can now be found using the wake-survey analysis method.[8–11] Such formulas currently include higher-order lift-and-drag corrections for powered-engine equipped models.[12,13]

In this paper the general lift-and-drag equations in the momentum integral forms are expanded into perturbation forms using the small perturbation method[14] to generalize Betz–Maskell's lift-and-drag

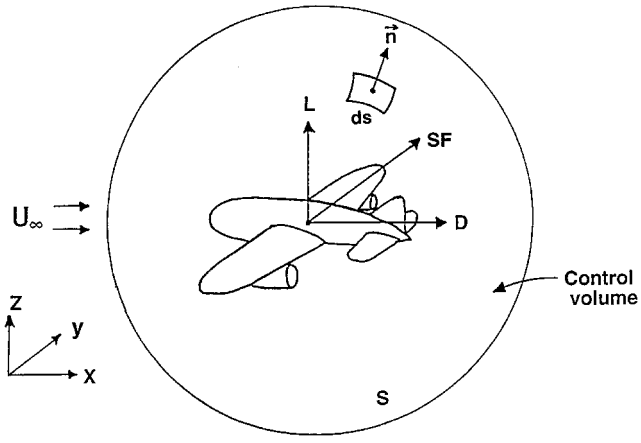

Fig. 1 Three components of body force acting on model.

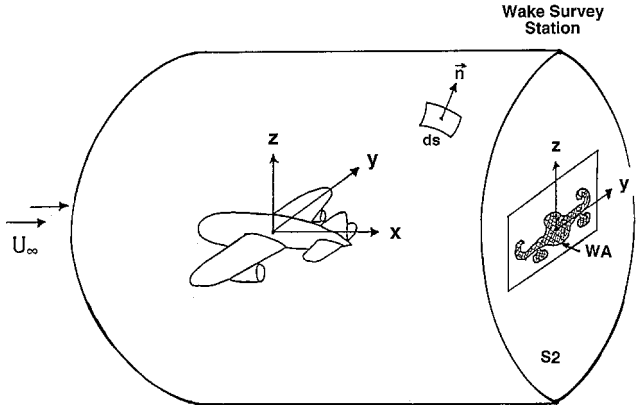

Fig. 2a Control volume and its coordinate system (free-air case).

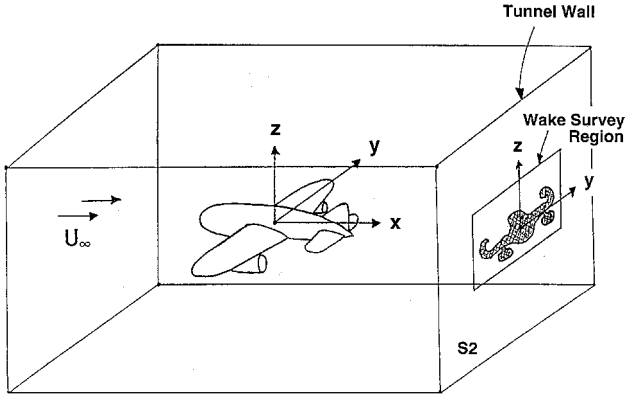

Fig. 2b Control volume and its coordinate system (with tunnel walls).

equations to cover compressible flows. New simpler and cleaner expansion procedures (compared to those in Refs. 11 and 12) are introduced to improve the accuracy in higher-order term calculations of these expanded lift-and-drag equations. It will thus be shown that both the lift and drag of an airplane model can be accurately calculated by simply measuring flow variables inside of the model wake region.

To evaluate the effects of the (currently developed) second-order correction terms on the model lift and drag, some wake-survey analysis results from previously published data[13,15] were recalculated. For the wake-survey data acquisitions and their reductions the Quantitative Wake-Survey System (QWSS)[5] was employed. The QWSS uses a single five-hole probe mounted on a continuously sweeping traverser to measure velocities and total pressure deficit inside the model wake region. The QWSS typically acquires wake data on over 50,000 data points in 10–15 min. Total temperature measurements will also be required when the wind tunnel model is equipped with powered engines.

Lift-and-Drag Equations

In general, the force acting on an airplane model $\boldsymbol{F}$ can be expressed, by applying the integral form of the momentum equations, as an integral over the surface of a control volume that contains the model.

$$\boldsymbol{F} = -\iint_S \rho \boldsymbol{u}(\boldsymbol{u}\cdot\boldsymbol{n})\,\mathrm{d}s - \iint_S P\boldsymbol{n}\,\mathrm{d}s + \iint_S \boldsymbol{\tau}\cdot\boldsymbol{n}\,\mathrm{d}s \tag{1}$$

where P, ρ, $\boldsymbol{u}[=(u, v, w)]$ and $\boldsymbol{\tau}$ are pressure, density, velocity vector, and viscous and turbulence stress tensor, respectively.

Knowing

$$\iint_S P_\infty \boldsymbol{n}\,\mathrm{d}s \left(= \iiint_V \nabla P_\infty\,\mathrm{d}v \right) = 0$$

for a closed control volume (applying Gauss's divergence theorem for a scalar function $P_\infty = \text{const}$), Eq. (1) can be rewritten as

$$\boldsymbol{F} = -\iint_S \rho \boldsymbol{u}(\boldsymbol{u}\cdot\boldsymbol{n})\,\mathrm{d}s - \iint_S (P - P_\infty)\boldsymbol{n}\,\mathrm{d}s + \iint_S \boldsymbol{\tau}\cdot\boldsymbol{n}\,\mathrm{d}s \tag{2}$$

Assuming that the x and z axes are aligned with the undisturbed freestream direction (direction of the drag) and direction of the lift, respectively, and that the remaining y axis is normal to both x and z axes (Fig. 1), the three components of the body force (drag, side force, and lift) can be expressed as $(D, S_F, L) = (\boldsymbol{F}\cdot\boldsymbol{I}_x, \boldsymbol{F}\cdot\boldsymbol{I}_y, \boldsymbol{F}\cdot\boldsymbol{I}_z)$. Note that $\boldsymbol{I}_x$, $\boldsymbol{I}_y$, and $\boldsymbol{I}_z$ are the unit vectors pointing in the x, y, and z directions, respectively.

If the control volume is sufficiently far from the model, the viscous force can be neglected, and Eq. (1) becomes

$$\boldsymbol{F} = -\iint_S \rho \boldsymbol{u}(\boldsymbol{u}\cdot\boldsymbol{n})\,\mathrm{d}s - \iint_S (P - P_\infty)\boldsymbol{n}\,\mathrm{d}s \tag{3}$$

Taking the z component of the force, lift L is calculated as

$$L = \boldsymbol{F}\cdot\boldsymbol{I}_z = -\iint_S \rho w(\boldsymbol{u}\cdot\boldsymbol{n})\,\mathrm{d}s - \iint_S (P - P_\infty)n_z\,\mathrm{d}s \tag{4}$$

Similarly for drag D,

$$D = \boldsymbol{F}\cdot\boldsymbol{I}_x = -\iint_S \rho u(\boldsymbol{u}\cdot\boldsymbol{n})\,\mathrm{d}s - \iint_S (P - P_\infty)n_x\,\mathrm{d}s \tag{5}$$

Expansion of Lift-and-Drag Equations

The problem with such momentum integral forms for model forces is that the integral must be evaluated over the entire surface of a control volume that contains the model. Betz[1] and Maskell[2] solved this problem by demonstrating that an integral formulation for forces acting on the model can be obtained (for incompressible flows) from flow variables measured within the model wake region, "wake integrals" (see Fig. 2).

In this section we will expand lift-and-drag equations (4) and (5) into perturbation forms for the purpose of extending the Betz and Maskell's wake integrals to cover compressible flows. We assume downstream states that differ only slightly from the state of approach,

$$u = U_\infty + \Delta u = U_\infty(1 + \Delta u/U_\infty) \tag{6}$$

$$P = P_\infty + \Delta P = P_\infty(1 + \Delta P/P_\infty) \tag{7}$$

$$\rho = \rho_\infty + \Delta\rho = \rho_\infty(1 + \Delta\rho/\rho_\infty) \tag{8}$$

where $|\Delta u/U_\infty|, |\Delta P/P_\infty|, |\Delta\rho/\rho_\infty| \ll 1$.

To relate the density and pressure perturbations $\Delta\rho$ and ΔP to the variables measured at the wake survey station, we employ the entropy equation[16,17]:

$$(s - s_\infty)/R \equiv \Delta s/R = 1/(\gamma - 1)\,\ell n(T/T_\infty) - \ell n(\rho/\rho_\infty) \quad (9)$$

Here we assumed that the gas is calorically perfect (constant specific heats C_v and C_p). Then, the energy equation for an airplane model equipped with powered engines (assuming a flow with Prandtl number unity) is used

$$h + (u^2 + v^2 + w^2)/2 = h_\infty + U_\infty^2/2 + \Delta H \quad (10)$$

to relate temperature to measured variables. ΔH is positive in the exhausts of the powered engines and is zero outside the engine exhausts (for a case without powered engines, $\Delta H \equiv 0$). It is also clear from Eq. (10) that our fundamental assumption $|\Delta u/U_\infty| \ll 1$ will be violated inside the engine exhausts when $|\Delta H/U_\infty^2|$ is much lager than one.

Solving the entropy equation (9) for density yields

$$\rho/\rho_\infty = e^{-(\Delta s/R)}(T/T_\infty)^{1/(\gamma-1)} \quad (11)$$

and using the equation of state $P = \rho RT$ the static pressure can be expressed in a similar explicit form:

$$P/P_\infty = e^{-(\Delta s/R)}(T/T_\infty)^{\gamma/(\gamma-1)} \quad (12)$$

Then, rewriting the energy equation (10), T/T_∞ can be expressed in a perturbation form:

$$\frac{T}{T_\infty} = 1 + \frac{\gamma-1}{2}M_\infty^2\left[-2\frac{\Delta u}{U_\infty} - \left(\frac{\Delta u}{U_\infty}\right)^2 - \left(\frac{v}{U_\infty}\right)^2 - \left(\frac{w}{U_\infty}\right)^2 + 2\frac{\Delta H}{U_\infty^2}\right] \quad (13)$$

Here, the definitions of enthalpy $h = C_pT = a^2/(\gamma-1)$ and speed of sound $a^2 = \gamma RT$ for the perfect gas have been used.

Substituting Eq. (13) into Eqs. (11) and (12), we are ready to expand the right-hand side (RHS) of these equations into small perturbation forms to obtain expressions for $\Delta\rho/\rho_\infty$ and $\Delta P/P_\infty$. Before the expansions, however, one must examine the orders of magnitude of v/U_∞, w/U_∞, $\Delta s/R$, and $\Delta H/U_\infty^2$, for the validation of expansions.

Order-of-Magnitude Estimations

As shown in Ref. 13 for a no-energy-added case ($\Delta H = 0$), the order-of-magnitude relations among $\Delta u/U_\infty$, v/U_∞, and w/U_∞ are $\mathcal{O}(\Delta u/U_\infty) \sim \mathcal{O}(v/U_\infty) \sim \mathcal{O}(w/U_\infty)$ inside of the model wake region and $\mathcal{O}(\Delta u/U_\infty) \sim \mathcal{O}[(v/U_\infty)^2] \sim \mathcal{O}[(w/U_\infty)^2]$ outside of the model wake region. Therefore, knowing that the order of magnitude of $\Delta u/U_\infty$ within the outside wake region is at most $\mathcal{O}(v/U_\infty)$ or $\mathcal{O}(w/U_\infty)$, the fundamental order relation

$$\mathcal{O}(\Delta u/U_\infty) \sim \mathcal{O}(v/U_\infty) \sim \mathcal{O}(w/U_\infty) \quad (14)$$

is still valid in the entire region of the wake-survey station. It is important, however, to remember that both our basic assumption $|\Delta u/U_\infty| \ll 1$ and the key relation (14) will not be valid for high-power engine setting cases.

Applying the small perturbation forms (7) and (8), for pressure and density, to modified entropy equation of (9)

$$\Delta s/C_v = \ell n(P/P_\infty) - \gamma\,\ell n(\rho/\rho_\infty)$$

one can obtain

$$\Delta s/C_v = \Delta P/P_\infty - \gamma(\Delta\rho/\rho_\infty) + \cdots$$

Then utilizing $C_v = R/(\gamma-1)$, we can see that the order of magnitude of $\Delta s/R$ is at most

$$\mathcal{O}(\Delta s/R) \sim \mathcal{O}(\Delta P/P_\infty), \mathcal{O}(\Delta\rho/\rho_\infty) \quad (15)$$

Similarly, to estimate the order of magnitude of $M_\infty^2\Delta h/U_\infty^2$ we use another form of entropy equation (9) (also see Ref. 18)

$$T_\infty\rho_\infty\Delta s = \rho_\infty\Delta h - \Delta P + \cdots$$

with the help of the equation of state $P_\infty = \rho_\infty RT_\infty$ and the definition of speed of sound $a_\infty^2 = \gamma RT_\infty$; we can rewrite the equation

$$M_\infty^2\left(\Delta h/U_\infty^2\right) = (1/\gamma)(\Delta P/P_\infty + \Delta s/R) + \cdots$$

where $\Delta h = h - h_\infty$. Hence, one can get

$$\mathcal{O}\left[M_\infty^2\left(\Delta h/U_\infty^2\right)\right] \sim \mathcal{O}(\Delta P/P_\infty), \mathcal{O}(\Delta s/R) \sim \mathcal{O}(\Delta P/P_\infty), \mathcal{O}(\Delta\rho/\rho_\infty) \quad (16)$$

In Eq. (16), relation (15) has been used.

Now employing the small perturbation form (6) for u, energy equation (10) can be rewritten as

$$M_\infty^2\frac{\Delta H}{U_\infty^2} = M_\infty^2\frac{\Delta h}{U_\infty^2} + M_\infty^2\frac{\Delta u}{U_\infty} + \frac{M_\infty^2}{2}\left[\left(\frac{\Delta u}{U_\infty}\right)^2 + \left(\frac{v}{U_\infty}\right)^2 + \left(\frac{w}{U_\infty}\right)^2\right] \quad (17)$$

Finally, combining the order relations given by Eqs. (14) and (16) to Eq. (17) we can conclude, for subsonic and transonic flows $\mathcal{O}(M_\infty^2) \sim 1$, that

$$\mathcal{O}\left[M_\infty^2\left(\Delta H/U_\infty^2\right)\right] \sim \mathcal{O}(\Delta u/U_\infty), \mathcal{O}(\Delta P/P_\infty), \mathcal{O}(\Delta\rho/\rho_\infty) \quad (18)$$

Density and Pressure Perturbations

Knowing that $|\Delta s/R|, |M_\infty^2\Delta H/U_\infty^2| \ll 1$ are valid (for subsonic and transonic flows) when our fundamental conditions $|\Delta u/U_\infty|, |\Delta P/P_\infty|, |\Delta\rho/\rho_\infty| \ll 1$ are satisfied, we are ready to expand the RHS of density and pressure equations (11) and (12):

$$e^{-(\Delta s/R)} = 1 - \Delta s/R + \tfrac{1}{2}(\Delta s/R)^2 + \cdots \quad (19)$$

Letting the temperature equation (13) be

$$T/T_\infty = 1 + [(\gamma-1)/2]M_\infty^2 K \quad (20)$$

where

$$K \equiv -2\frac{\Delta u}{U_\infty} + 2\frac{\Delta H}{U_\infty^2} - \left(\frac{\Delta u}{U_\infty}\right)^2 - \left(\frac{v}{U_\infty}\right)^2 - \left(\frac{w}{U_\infty}\right)^2 \quad (21)$$

and knowing $|(\gamma-1)M_\infty^2 K/2| \ll 1$ for subsonic and transonic flows [$\mathcal{O}(M_\infty^2) \sim 1$], temperature terms in Eqs. (11) and (12) can be also expanded

$$\left(\frac{T}{T_\infty}\right)^{1/(\gamma-1)} = 1 + \frac{1}{\gamma-1}\left(\frac{\gamma-1}{2}M_\infty^2 K\right) + \frac{1}{2}\left(\frac{1}{\gamma-1}\right)\left(\frac{1}{\gamma-1} - 1\right)\left(\frac{\gamma-1}{2}M_\infty^2 K\right)^2 + \cdots$$

$$= 1 - M_\infty^2\frac{\Delta u}{U_\infty} + M_\infty^2\frac{\Delta H}{U_\infty^2} - \frac{M_\infty^2}{2}\left\{\left[1 - (2-\gamma)M_\infty^2\right]\left(\frac{\Delta u}{U_\infty}\right)^2 + \left(\frac{\Delta v}{U_\infty}\right)^2 + \left(\frac{\Delta w}{U_\infty}\right)^2\right\} + \frac{2-\gamma}{2}M_\infty^4\left(\frac{\Delta H}{U_\infty^2}\right)^2 - (2-\gamma)M_\infty^4\frac{\Delta u}{U_\infty}\frac{\Delta H}{U_\infty^2} + \mathcal{O}(\Delta^3) \quad (22)$$

where $\mathcal{O}(\Delta^3)$ denotes the third- and higher-order terms. Similarly, one can obtain

$$\left(\frac{T}{T_\infty}\right)^{\gamma/(\gamma-1)} = 1 - \gamma M_\infty^2 \frac{\Delta u}{U_\infty} + \gamma M_\infty^2 \frac{\Delta H}{U_\infty^2} - \frac{\gamma}{2} M_\infty^2 \left[\left(1 - M_\infty^2\right) \left(\frac{\Delta u}{U_\infty}\right)^2 + \left(\frac{\Delta v}{U_\infty}\right)^2 + \left(\frac{\Delta w}{U_\infty}\right)^2 \right] + \frac{\gamma}{2} M_\infty^4 \left(\frac{\Delta H}{U_\infty^2}\right)^2 - \gamma M_\infty^4 \frac{\Delta u}{U_\infty} \frac{\Delta H}{U_\infty^2} + \mathcal{O}(\Delta^3) \tag{23}$$

Substituting Eqs. (19) and (22) into Eq. (11), we can obtain the density perturbation $\Delta\rho/\rho_\infty$ as

$$\frac{\Delta\rho}{\rho_\infty} = -M_\infty^2 \frac{\Delta u}{U_\infty} - \frac{1}{2} M_\infty^2 \left\{ \left[1 - (2-\gamma) M_\infty^2\right] \left(\frac{\Delta u}{U_\infty}\right)^2 + \left(\frac{v}{U_\infty}\right)^2 + \left(\frac{w}{U_\infty}\right)^2 - 2\frac{\Delta H}{U_\infty^2} \right\} - \frac{\Delta s}{R} + \frac{1}{2}\left(\frac{\Delta s}{R}\right)^2 + M_\infty^2 \frac{\Delta u}{U_\infty} \frac{\Delta s}{R} - M_\infty^2 \frac{\Delta s}{R} \frac{\Delta H}{U_\infty^2} + \frac{2-\gamma}{2} M_\infty^4 \left(\frac{\Delta H}{U_\infty^2}\right)^2 - (2-\gamma) M_\infty^4 \frac{\Delta u}{U_\infty} \frac{\Delta H}{U_\infty^2} + \mathcal{O}(\Delta^3) \tag{24}$$

Similarly, substitution of Eqs. (19) and (23) into Eq. (12) yields pressure perturbation

$$\frac{\Delta P}{P_\infty} = -\gamma M_\infty^2 \frac{\Delta u}{U_\infty} - \frac{\gamma}{2} M_\infty^2 \left[\left(1 - M_\infty^2\right) \left(\frac{\Delta u}{U_\infty}\right)^2 + \left(\frac{v}{U_\infty}\right)^2 + \left(\frac{w}{U_\infty}\right)^2 - 2\frac{\Delta H}{U_\infty^2} \right] - \frac{\Delta s}{R} + \frac{1}{2}\left(\frac{\Delta s}{R}\right)^2 + \gamma M_\infty^2 \frac{\Delta u}{U_\infty} \frac{\Delta s}{R} - \gamma M_\infty^2 \frac{\Delta s}{R} \frac{\Delta H}{U_\infty^2} + \frac{\gamma}{2} M_\infty^4 \left(\frac{\Delta H}{U_\infty^2}\right)^2 - \gamma M_\infty^4 \frac{\Delta u}{U_\infty} \frac{\Delta H}{U_\infty^2} + \mathcal{O}(\Delta^3) \tag{25}$$

From Eqs. (24) and (25) it can be seen that the orders of magnitude of $\Delta\rho/\rho_\infty$ and $\Delta P/P_\infty$ are the same as that of $\Delta u/U_\infty$ for subsonic and transonic flows.

Lift Analysis

With the help of the density and pressure perturbations derived in the preceding section, lift integral (4) is ready to be expanded into a small perturbation form. Employing the small perturbation forms (6), (7), and (8), the integrands of lift equation (4) can be rewritten as

$$\rho w(\boldsymbol{u}\cdot\boldsymbol{n}) = \rho w u n_x + \rho w v n_y + \rho w^2 n_z = \rho_\infty U_\infty w \times (1 + \Delta\rho/\rho_\infty)[(1 + \Delta u/U_\infty) n_x + (v/U_\infty) n_y + (w/U_\infty) n_z] \tag{26}$$

and

$$(P - P_\infty) n_z = \Delta P n_z \tag{27}$$

After substituting these equations into the lift equation (4) with the help of Eqs. (24) and (25), we push out control surface S to a distance far from the model, while holding the wake-survey plane S_2 at a finite (downstream) distance from the model (see Fig. 2a). Then, following the similar arguments given in Ref. 13, it can be shown that

$$L = \rho_\infty U_\infty \iint_{W_A} y\xi \, \mathrm{d}s - \rho_\infty U_\infty^2 \left(1 - M_\infty^2\right) \iint_{S_2} \frac{w}{U_\infty} \frac{\Delta u}{U_\infty} \mathrm{d}s + M_\infty^2 \frac{\gamma P_\infty}{R} \iint_{W_A} \frac{w}{U_\infty} \Delta s \, \mathrm{d}s - \rho_\infty M_\infty^2 \iint_{W_A} \frac{w}{U_\infty} \Delta H \, \mathrm{d}s + \mathcal{O}(\Delta^3) \tag{28}$$

In Eq. (28) ξ denotes the x component of vorticity vector $\nabla \times \boldsymbol{u}$. The symbol W_A indicates an integral over the model wake region on S_2 (see Fig. 2a). Knowing that ΔH, Δs, and ξ are zero outside the model wake region, the lift integrals in Eq. (28) are expressed in wake integrals except for the second integral. However, it has been shown by Kusunose[13] that the major contribution on this second integral comes from the integration over the model wake region, or

$$\iint_{S_2} \frac{w}{U_\infty} \frac{\Delta u}{U_\infty} \mathrm{d}s = \iint_{W_A} \frac{w}{U_\infty} \frac{\Delta u}{U_\infty} \mathrm{d}s + \mathcal{O}(\Delta^3) \tag{29}$$

Then, all of the lift integrals in Eq. (28), finally, become wake integrals, except for the third-and higher-order small terms

$$L = \rho_\infty U_\infty \iint_{W_A} y\xi \, \mathrm{d}s - \rho_\infty U_\infty^2 \left(1 - M_\infty^2\right) \iint_{W_A} \frac{w}{U_\infty} \frac{\Delta u}{U_\infty} \mathrm{d}s + M_\infty^2 \frac{\gamma P_\infty}{R} \iint_{W_A} \frac{w}{U_\infty} \Delta s \, \mathrm{d}s - \rho_\infty M_\infty^2 \iint_{W_A} \frac{w}{U_\infty} \Delta H \, \mathrm{d}s + \mathcal{O}(\Delta^3) \tag{30}$$

For incompressible flows ($M_\infty \to 0$) the lift equation reduces to

$$L = \rho_\infty U_\infty \iint_{W_A} y\xi \, \mathrm{d}s - \rho_\infty U_\infty^2 \iint_{W_A} \frac{w}{U_\infty} \frac{\Delta u}{U_\infty} \mathrm{d}s + \mathcal{O}(\Delta^3) \tag{31}$$

The leading-order term of the lift equation, as we expected, turns out to be identical to the streamwise vorticity integral in the far field, which was first obtained by Maskell in 1972 (Ref. 2). However, the second-order (lift correction) term does not agree with that of the Maskell's equation.

$$L_{\text{Maskell}} = \rho_\infty U_\infty \iint_{W_A} y\xi \, \mathrm{d}s + \rho_\infty \iint_{W_A} (u^* - u) w \, \mathrm{d}s + \cdots \tag{32}$$

The results given in Ref. 13 revealed that the current second-order correction outperforms Maskell's correction.

Drag Analysis

To take into account the effect of wind-tunnel walls on the model drag, some of the control-volume surfaces are replaced by tunnel walls (Fig. 2b). Applying the integral form of the continuity equation to drag equation (5) and assuming that tunnel walls are solid and parallel, the drag equation with tunnel walls, as shown in Ref. 12, reduces to

$$D = \iint_{S_2} [\rho u (U_\infty - u) + (P_\infty - P)] \, \mathrm{d}y \, \mathrm{d}z - \dot{m} U_\infty \tag{33}$$

Using Eqs. (6) and (8), ρu can be rewritten as

$$\frac{\rho u}{\rho_\infty U_\infty} = \left(1+\frac{\Delta\rho}{\rho_\infty}\right)\left(1+\frac{\Delta u}{U_\infty}\right) = 1+\frac{\Delta u}{U_\infty}+\frac{\Delta\rho}{\rho_\infty}+\frac{\Delta u}{U_\infty}\frac{\Delta\rho}{\rho_\infty} \tag{34}$$

Similarly, writing $P_\infty - P$ term in a perturbation form, $P_\infty - P = -P_\infty(\Delta P/P_\infty)$, and utilizing the density and pressure perturbation equations (24) and (25), drag equation (33) can be expressed as

$$\begin{aligned} D = &\iint_{W_A} P_\infty \frac{\Delta s}{R}\,\mathrm{d}y\,\mathrm{d}z + \iint_{S_2} \frac{\rho_\infty}{2}(v^2+w^2)\,\mathrm{d}y\,\mathrm{d}z \\ &- \iint_{W_A} \rho_\infty \Delta H\,\mathrm{d}y\,\mathrm{d}z - \dot{m}U_\infty \\ &- \iint_{S_2} \frac{\rho_\infty}{2}\left(1-M_\infty^2\right)(\Delta u)^2\,\mathrm{d}y\,\mathrm{d}z \\ &- \iint_{W_A} \frac{P_\infty}{2}\left(\frac{\Delta s}{R}\right)^2 \mathrm{d}y\,\mathrm{d}z \\ &+ \iint_{W_A} \rho_\infty \Delta H\left(\frac{\Delta s}{R} - \frac{M_\infty^2}{2}\frac{\Delta H}{U_\infty^2}\right)\mathrm{d}y\,\mathrm{d}z + \mathcal{O}(\Delta^3) \end{aligned} \tag{35}$$

In Eq. (35) the condition that Δs and ΔH are zero outside of the model wake region has been used. Our drag equation (35) is almost identical to that of van der Vooren and Slooff,[19] except that the current drag equation does not have a singular behavior when M_∞ approaches to zero.

For the purposes of developing a practical wake-survey analysis method, the current drag equation (35) is not suitable because the second (induced drag) and fourth integrals are not wake integrals. They must be evaluated over the entire downstream cross section S_2. Fortunately, this problem has been solved by Maskell[2] and Cummings et al.[10] Maskell introduced the idea of defining scalar functions $\psi(y,z)$ and $\phi(y,z)$ for the cross-sectional velocities (v and w) to reduce the induced drag integral to a wake integral. ψ and ϕ are related to the trailing vorticity and the velocity gradient through the Poisson equations $\nabla^2\psi = -\xi$ and $\nabla^2\phi = \sigma$, respectively, where ξ and σ denote the x-component vorticity vector of $\nabla\times\boldsymbol{u}$, $\partial w/\partial y - \partial v/\partial z$, and $-\partial u/\partial x$, respectively.

Using a result from Cummings et al.,[10] it can be shown that the second integral and the fourth integral in Eq. (35) relate to Maskell's drag integral[2] as

$$\begin{aligned} &\iint_{S_2} \frac{\rho_\infty}{2}(v^2+w^2)\,\mathrm{d}y\,\mathrm{d}z - \iint_{S_2} \frac{\rho_\infty}{2}\left(1-M_\infty^2\right)(\Delta u)^2\,\mathrm{d}y\,\mathrm{d}z \\ &\quad = \frac{\rho_\infty}{2}\iint_{W_A} \psi\xi\,\mathrm{d}y\,\mathrm{d}z + \mathcal{O}(\Delta^3) \end{aligned} \tag{36}$$

Combining Eqs. (36) and (35), we can finally obtain a drag equation in which all of the drag components are reduced to wake integrals (except for the third-and higher-order small terms):

$$\begin{aligned} D = &\iint_{W_A} P_\infty \frac{\Delta s}{R}\,\mathrm{d}y\,\mathrm{d}z + \iint_{W_A} \frac{\rho_\infty}{2}\psi\xi\,\mathrm{d}y\,\mathrm{d}z \\ &- \iint_{W_A} \rho_\infty \Delta H\,\mathrm{d}y\,\mathrm{d}z - \dot{m}U_\infty - \iint_{W_A} \frac{P_\infty}{2}\left(\frac{\Delta s}{R}\right)^2 \mathrm{d}y\,\mathrm{d}z \\ &+ \iint_{W_A} \rho_\infty \Delta H\left[\frac{\Delta s}{R} - \frac{M_\infty^2}{2}\frac{\Delta H}{U_\infty^2}\right]\mathrm{d}y\,\mathrm{d}z + \mathcal{O}(\Delta^3) \end{aligned} \tag{37}$$

From Eqs. (30) and (37) it has been shown that both the lift and drag of an airplane model can be calculated accurately by simply measuring flow variables inside of the model wake region. This is a key result to allow for the practical application of quantitative wake surveys for accurate lift-and-drag predictions for airplane models.

Here, it is important to note that the Maskell's drag integral given by the RHS of Eq. (36) does not represent the "traditional" induced drag that is defined by the second integral in Eq. (35). However, his drag integral has been commonly used in the wake-survey analysis method to predict the induced drag of airplane models.[2–12] For the purpose of distinguishing Maskell's induced drag integral from the traditional induced drag integral, Maskell's is denoted as "Maskell's induced drag" throughout this paper.

For bookkeeping purposes the first and second terms of the drag equation (37) are considered the "profile" and Maskell's induced drag (D_p and D_{Mi}), respectively. The third and fourth terms are extra terms resulting from powered engine effects, and they represent "(added) enthalpy"[9,10] and "injected mass" effects on drag (D_e and D_m), respectively. All of the remaining terms in Eq. (37) are simply denoted as D_{ct}, a drag correction term, for the sake of convenience. For an airplane model equipped with high-power engines, our small perturbation assumptions will not be valid in high-speed jet exhaust regions. A drag calculation method for a model with high-power engines will be discussed in the Appendix.

Profile and Enthalpy Drag

Using the entropy equation (9) and recalling that the stagnation entropy is simply equal to the entropy of the state considered,[16,18] the entropy change can be expressed as

$$\Delta s = C_p \ln\left(T_T/T_{T_\infty}\right) - R\ln\left(P_T/P_{T_\infty}\right) \tag{38}$$

With a calorically perfect gas the change in the total (or stagnation) enthalpy can also be written as

$$\Delta H = h_T - h_{T_\infty} = C_p\left(T_T - T_{T_\infty}\right) \tag{39}$$

Substituting Eqs. (38) and (39) into the profile and enthalpy drag equations defined in Eq. (37) yields[12]

$$D_p = P_\infty \iint_{W_A} \left(\frac{\gamma}{\gamma-1}\ln\frac{T_T}{T_{T_\infty}} - \ln\frac{P_T}{P_{T_\infty}}\right)\mathrm{d}y\,\mathrm{d}z \tag{40}$$

$$D_e = -P_\infty\frac{\gamma}{\gamma-1}\left(1+\frac{\gamma-1}{2}M_\infty^2\right)\iint_{W_A}\left(\frac{T_T}{T_{T_\infty}}-1\right)\mathrm{d}y\,\mathrm{d}z \tag{41}$$

Because total temperature T_T differs from T_{T_∞} only in the powered engine exhaust regions, the total temperature measurements over the entire region of the model wake is not necessary.

From Eqs. (40) and (41) it can be seen that the total temperature terms in the profile and enthalpy drag equations will cancel each other for low-subsonic flows $M_\infty \simeq 0$, and the sum of the two equations reduces to a total pressure deficit[12]

$$(D_p + D_e)_{M_\infty\to 0} = \iint_{W_A}\left(P_{T_\infty} - P_T\right)\mathrm{d}y\,\mathrm{d}z + \cdots \tag{42}$$

The total temperature, therefore, will not play a major role in the drag analysis for low-subsonic flows. Without the supply of the external work, both the enthalpy drag D_e and the total temperature contribution to the profile drag will vanish.

Wave Drag Extraction from Profile Drag

For transonic flows it is important to recognize two different types of entropy production mechanisms that exist within the flowfield around the model. The first results from the fluid particle flowing though (viscous) rotational layers (for example, boundary layers

and vortical wakes). The second is caused by the fluid particle flowing through shock waves. Here, the vortical wake is defined by the wake originating from boundary layers that have developed along the model surfaces (see Fig. 3). Because a normal shock does not generate vorticity in the downstream flowfield, it is reasonable, then, to assume that the downstream flow through a weakly curved shock generated by a typical transonic transport airplane is nearly irrotational and therefore $\boldsymbol{u} \times \boldsymbol{\omega} \simeq 0$.

For separating the model wake into its shock wake and its vortical wake portions (see Fig. 3), it is critical to note that the vector product $\boldsymbol{u} \times \boldsymbol{\omega}$ will never vanish along the entire region of the vortical wake.[15] Consequently, the shock wake and the vortical wake portions of the model wake are separable by checking the magnitude of $\boldsymbol{u} \times \boldsymbol{\omega}$. To illustrate this concept, a total pressure contour of a wing wake, including the shock wake, and the x component of vorticity vector ξ field in that wake are plotted in Figs. 4 and 5, respectively.[15]

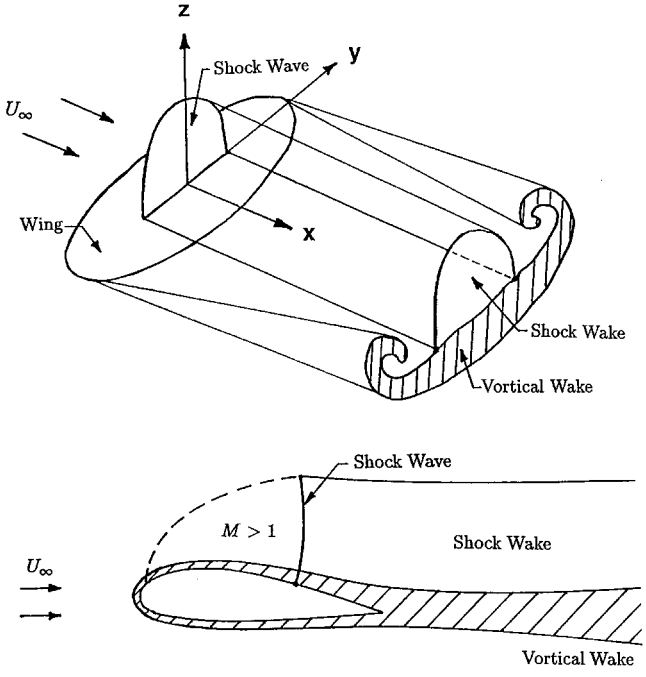

Fig. 3 Wing wake formation and its evolution.

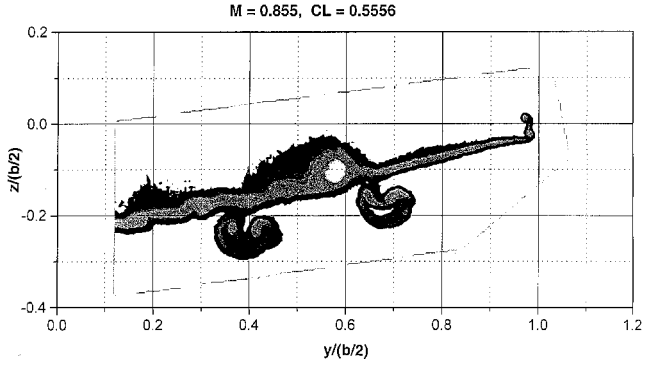

Fig. 4 Total pressure contours of a wing wake, including shock wake.

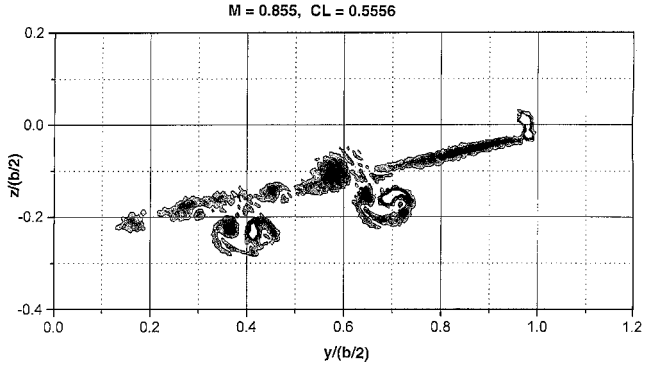

Fig. 5 *X*-component vorticity contours of a wing wake.

Maskell's Induced Drag

Maskell's induced drag integral

$$D_{\mathrm{Mi}} = \frac{\rho_\infty}{2} \iint_{W_A} \psi \xi \, \mathrm{d}y \, \mathrm{d}z \tag{43}$$

is commonly used in wake-survey analysis method.[2–12] As noted briefly in the preceding section, a Poisson equation $\nabla^2 \psi = -\xi$ should be solved for Maskell's scalar function $\psi(y, z)$ with the boundary condition $\psi = 0$ evaluated along the tunnel intersection[2,20] (see Fig. 2b). Outside of the model wake region W_A, $\xi = 0$.

For the "free-air" case (without interference of tunnel walls) the boundary condition $\psi = 0$ should be evaluated at $y^2 + z^2 \to \infty$, and Maskell's scalar function ψ can be expressed in the following simple analytical form.[9–11]

$$\psi(y, z) = -\frac{1}{4\pi} \iint_{W_A} \xi(y_0, z_0) \ln\left[(y - y_0)^2 + (z - z_0)^2\right] \mathrm{d}y_0 \, \mathrm{d}z_0 \tag{44}$$

Currently, the Poisson equation system is solved in two different ways. In the first approach the system is solved numerically, using a fast Poisson solver developed by L. B. Wigton of Boeing Enabling Technology Research (personal communications, January–February 2001, Seattle, WA). In the second approach the system of equations is solved analytically, utilizing Green's function method discussed in Ref. 11 in order to handle both the cases with and without tunnel walls.

Unfortunately, after Maskell introduced his induced drag integral (43), it has been difficult to understand the true physical meaning behind his induced drag integral. To investigate the physical properties owned by Maskell's induced drag integral, some studies were conducted in Ref. 21, and the reasons as to why Maskell's induced drag integral outperforms that from the lifting line theory were also discussed there.

Drag Correction Terms

Traditionally, higher-order drag correction terms are neglected in the wake-survey analysis method to allow the drag to be estimated with a wake integral. Because the current analysis demonstrates that all of the second-order drag correction terms in D_{ct}, as shown in Eq. (37), can be reduced to wake integrals, it is not necessary for them to be neglected. It might be advisable to retain those second-order correction terms for the sake of completeness of the theory.

Results and Discussion

To evaluate the second-order lift-and-drag correction terms given in Eqs. (30) and (37), the wake-survey data used in Refs. 13 and 15 (for nonpowered engine cases $\Delta H = 0$, and $\dot{m} = 0$) are reanalyzed. The currently developed wake-survey analysis method has been implemented as a part of the QWSS[5] to extract spanwise lift-and-drag distributions as well as total lift and drag of the models, in addition to contours of vorticity and total pressure at the wake survey station. Because the primary focus of this document is to develop new lift-and-drag formulas and their validations, the experimental setup of the tests, as well as the complete test results, will not be discussed.

Lift Predictions

To demonstrate the accuracy of our new lift prediction capability, the NASA LRC450 test data from Ref. 13 are selected. The wakes generated behind two transonic transport models (config. 1 and 2) during landing conditions at realistic low subsonic speeds

($M_\infty = 0.20$) were measured. Models were mounted on an island support type strut. Wake-survey data were obtained at several downstream stations in order to study overall characteristics of the model wake. The typical vorticity and total pressure contours at two different wake survey stations (x_{ws}) are shown in Figs. 6 and 7, in order to demonstrate the downstream growth of the wakes formed behind an airplane model (including the model support strut). It can be seen that the model strut has little effect on the generation of the x component of the vorticity vector (therefore, also on the model lift), but it is responsible for a large increment in the total pressure deficit at the far field. Because the model wake and the strut wake are mixed and are not separable at the far field, the drag estimations based on the far wake measurements are not recommended. Figure 8 shows the section lifts along the wake span at two different wake-survey stations. As the wake evolves downstream, the curves are smoothed out, and the detail in lift distribution on the wing is lost.

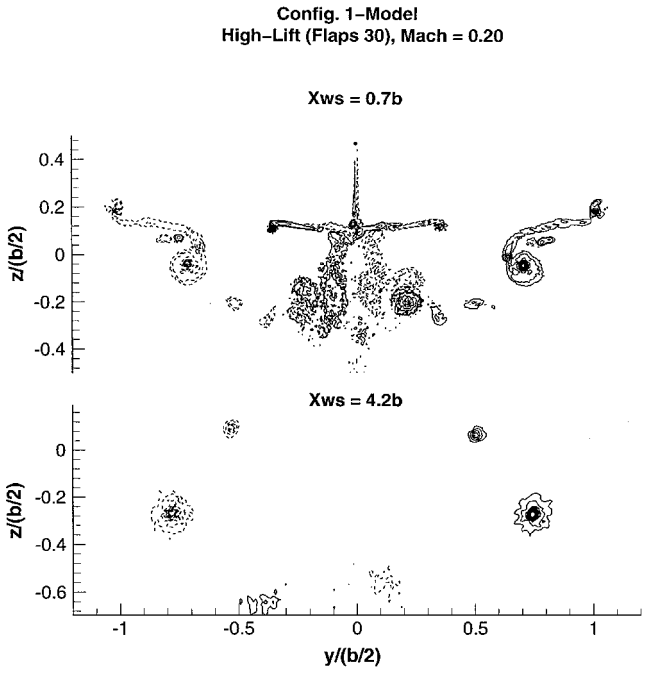

Fig. 6 Evolution of model wake (vorticity contours).

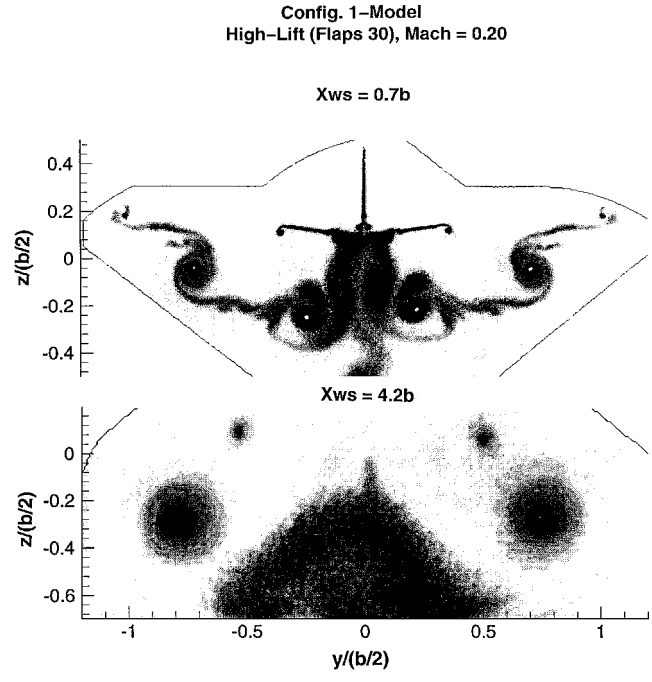

Fig. 7 Evolution of model wake (total pressure contours).

Table 1 Effects of lift correction term on lift config. 1-model, low-speed NASA/LaRC 14 × 22 test (LRC450)

Balance			Wake survey					
Mach	Flaps	C_{Lbl}[a]	X_{WS}[b]	C_L[c]	C_{Lwo}[d]	C_{Lvc}[e]	C_{Lec}[f]	Note
0.20	F30	1.3419	0.7b[g]	1.3534	1.3686	−0.0147	−0.0005	Landing
0.20	F30	1.3412	0.7b	1.3422	1.3572	−0.0146	− 0.0005	Landing
0.20	F30	1.3397	0.7b	1.3467	1.3644	−0.0172	−0.0005	Landing
0.20	F30	1.3371	4.2b	1.3597	1.3722	−0.0120	−0.0005	Landing
0.26	Up	0.5195	0.7b	0.5521	0.5566	−0.0042	−0.0003	Flap-up
0.26	Up	0.5202	4.2b	0.5614	0.5650	−0.0033	−0.0003	Flap-up

[a]bl: balance.
[b]X_{ws}: wake survey station.
[c]$C_L = C_{Lwo} + C_{Lvc} + C_{Lec}$.
[d]C_{Lwo}: C_L without corrections.
[e]C_{Lvc}: velocity correction.
[f]C_{Lec}: entropy correction.
[g]b: wing span.

Table 2 Effects of lift correction term on lift config. 2-model, low-speed NASA/LaRC 14 × 22 test (LRC450)

Balance			Wake survey					
Mach	Flaps	C_{Lbl}[a]	X_{WS}[b]	C_L[c]	C_{Lwo}[d]	C_{Lvc}[e]	C_{Lec}[f]	Note
0.20	F30	1.3209	0.7b[g]	1.3330	1.3455	−0.0120	−0.0005	Landing
0.20	F30	1.3224	0.7b	1.3401	1.3534	−0.0127	−0.0006	Landing
0.20	F30	1.3140	2.2b	1.3304	1.3402	−0.0094	−0.0004	Landing
0.20	F30	1.3222	2.2b	1.3375	1.3477	−0.0098	−0.0004	Landing
0.26	Up	0.4998	0.7b	0.5318	0.5351	−0.0030	−0.0003	Flap-up
0.26	Up	0.5003	2.2b	0.5158	0.5196	−0.0035	−0.0003	Flap-up

[a]bl: balance.
[b]X_{ws}: wake survey station.
[c]$C_L = C_{Lwo} + C_{Lvc} + C_{Lec}$.
[d]C_{Lwo}: C_L without corrections.
[e]C_{Lvc}: velocity correction.
[f]C_{Lec}: entropy correction.
[g]b: wing span.

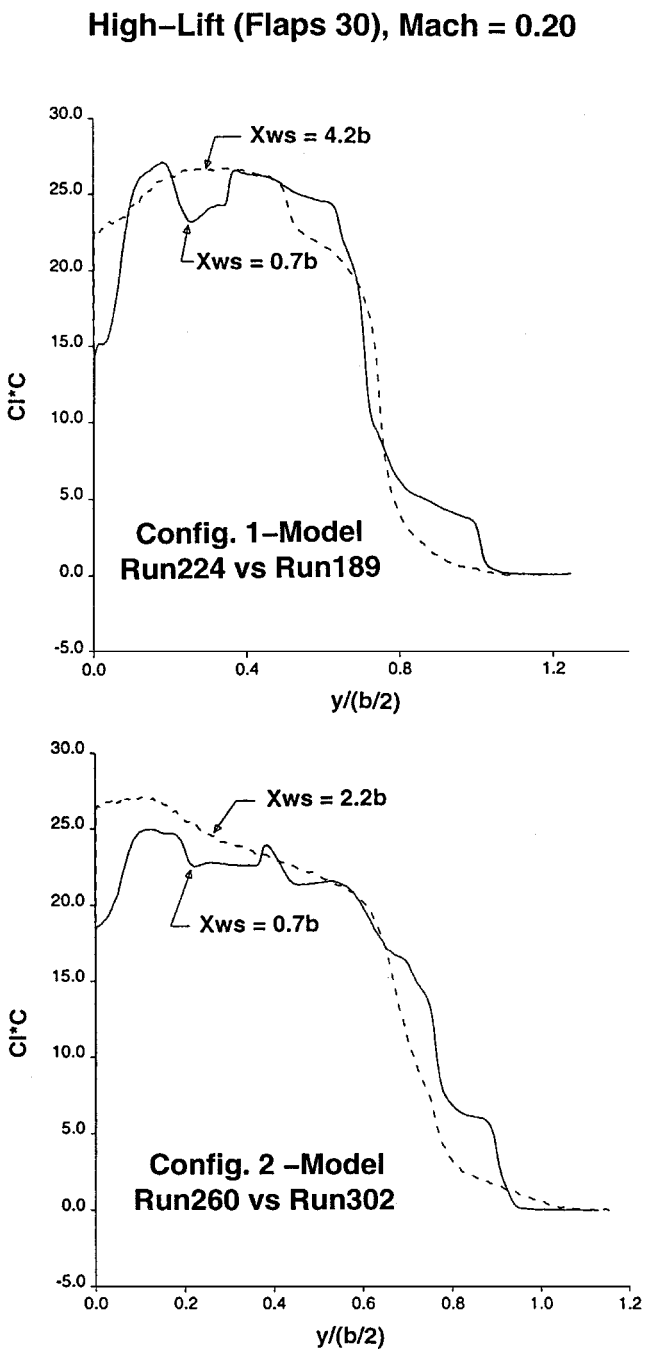

Fig. 8 Spanwise lift distributions at different wake-survey stations.

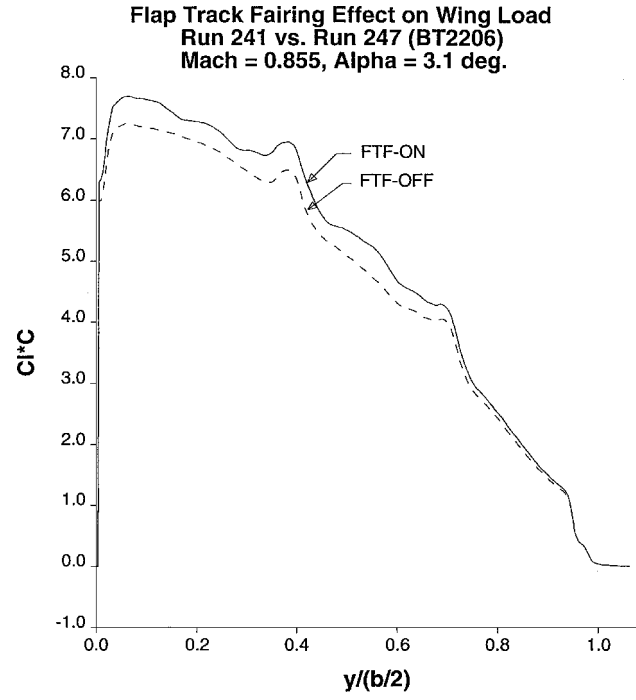

Fig. 9 Spanwise lift distributions (alpha = const).

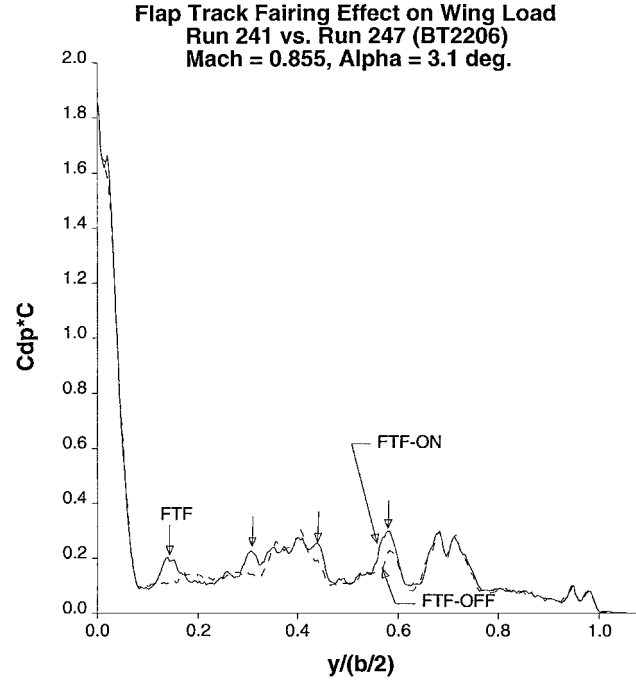

Fig. 10 Profile drag distributions (alpha = const).

Lifts calculated from the first-order approximation and with the second-order correction terms given in Eq. (30) are then compared to the wind-tunnel balance data for the config. 1 model and the config. 2 model in Tables 1 and 2, respectively. The symbols C_{Lwo}, C_{Lvc}, and C_{Lec} represent the lift coefficients corresponding to the first, second, and third integrals in Eq. (30), respectively, and C_L is the sum of these three lift coefficients. The predicted lift with correction terms C_L agrees with the balance data better than that without correction terms C_{Lwo}. Also, the results show that the measured lift is nearly independent of wake-survey locations, despite large apparent differences in the wake properties, as shown in Figs. 6 and 7.

Drag Predictions

For validation purposes of the current drag prediction capability at transonic speeds, some test data are selected from Ref. 15, where the effect of flap track fairings (FTFs) on the airplane drag was studied. A typical transonic transport configuration was selected to evaluate the suitability of the QWSS for detecting the minute changes in the drag for the changes in model configurations and model incidence angles.

During the test, the wake-survey plane was chosen close to the aft end of the fuselage, and the entire right half of the model wake was measured. Some wake-survey results for FTF-on and -off conditions are compared at $M_\infty = 0.855$ with fixed body angle of attack in Figs. 9, 10, and 11. As seen in Fig. 9, the effect of removing the FTFs from the lower surface of the wing is to cause a slight decrease in overall lift. This is probably because of a loss of effective camber to the wing surface. The effects of the four individual FTFs on the spanwise profile and induced drag are clearly captured in Figs. 10 and 11.

Table 3 FTF effect on drag high-speed model test, Mach = 0.855

Balance			Wake survey					
Alpha	C_{Lbl}[a]	C_{Dbl}	C_L	C_D[b]	C_{Dpr}[c]	C_{Dimk}[d]	C_{Dec}[e]	Note
3.1	0.4770	0.03207	0.4870	0.03113	0.02150	0.01040	−0.00077	FTF-ON
3.1	0.4756	0.03187	0.4947	0.03140	0.02145	0.01071	−0.00076	FTF-ON
3.1	0.4493	0.02978	0.4658	0.02922	0.02045	0.00951	−0.00073	FTF-OFF
3.3	0.4770	0.03154	0.4929	0.03111	0.02130	0.01057	−0.00076	FTF-OFF
3.3	0.4751	0.03157	0.4932	0.03088	0.02109	0.01054	−0.00075	FTF-OFF

[a]bl: balance.
[b]$C_D = C_{\mathrm{Dpr}} + C_{\mathrm{Dimk}} + C_{\mathrm{Dec}}$.
[c]pr: profile.
[d]imk: induced (Maskell's).
[e]ec: entropy correction.

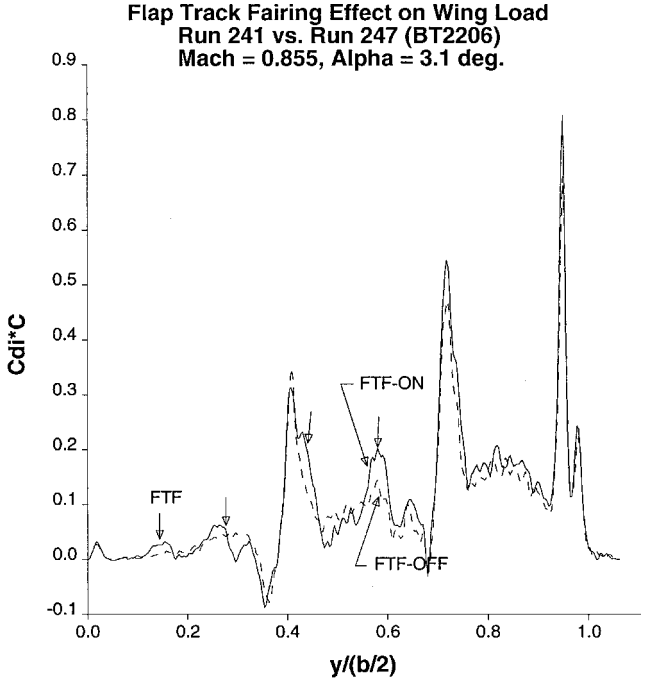

Fig. 11 Maskell's induced drag distributions (alpha = const).

Table 3 shows the comparisons of wake-integrated lift-and-drag values to the balance data for FTF-on and -off conditions (including some repeat-survey results). C_{Dpr}, C_{Dimk}, and C_{Dec} are the drag coefficients corresponding to the first, second, and fourth drag integrals in Eq. (37), and C_D is the total of these three coefficients. As shown in Table 3, the wake-integrated lift and drag agree with the balance to within a few percentage points, and the drag increments from both the lift and model configuration (FTF-on and -off) changes are accurately predicted.

Conclusions

To generalize Betz–Maskell's lift-and-drag equations for compressible flows, the lift-and-drag equations in the momentum integral forms were expanded into small perturbation forms. As a consequence, the original Betz–Maskell's lift-and-drag equation, including their higher-order correction terms, were extended to cover compressible flows. It was also shown that both the lift and drag can be calculated accurately without measuring flow variables outside of the model wake region. This result was critical to make quantitative wake surveys practical for accurate lift-and-drag predictions of airplane models. To study the effects of the currently proposed second-order correction terms on the model lift and drag, some wake-survey analysis results from previously published data were recalculated. The magnitudes of these correction terms were, as we expected, very small. Both the lift and the drag of airplane models were accurately predicted (compared with the wind-tunnel balance data) without measuring flow variables outside of the model wake region.

Appendix: High-Speed Jet Wakes

For a model equipped with high-power engines, our small perturbation assumptions, $|\Delta u/U_\infty|$, $|\Delta P/P_\infty|$, $|\Delta\rho/\rho_\infty| \ll 1$, will not be valid in high-speed jet exhaust regions. If a wake-survey station is chosen reasonably far from the model, the model wake can be divided into two different types of wake regions. One is the singular (jet wake) region in which the small perturbation method will break down, and the other is the regular wake region where our small perturbation assumptions are still valid. Typically, jet wakes can be found in small confined jet (or propeller) exhaust regions.

To search for jet wakes, we check the perturbation velocity $\Delta u/U_\infty$. If the value of the perturbation velocity exceeds a certain value (for example, $\Delta u/U_\infty \geq 0.2$), this point is considered to be in a jet wake. Then, we can divide the integral area S_2 of the drag integral (33) into two regions: jet wake regions $W_{A\,\mathrm{jet}}$ and regular wake regions $S_2 - W_{A\,\mathrm{jet}}$.

$$
\begin{aligned}
D &= \iint_{S_2} [\rho u(U_\infty - u) + (P_\infty - P)]\,\mathrm{d}y\,\mathrm{d}z - \dot{m}U_\infty \\
&= \iint_{W_{A\,\mathrm{jet}}} [\rho u(U_\infty - u) + (P_\infty - P)]\,\mathrm{d}y\,\mathrm{d}z \\
&\quad + \iint_{S_2 - W_{A\,\mathrm{jet}}} [\rho u(U_\infty - u) + (P_\infty - P)]\,\mathrm{d}y\,\mathrm{d}z - \dot{m}U_\infty \\
&= D_{\mathrm{jet}} + D_{\mathrm{reg}}
\end{aligned} \tag{45}
$$

where D_{jet} and D_{reg} have been defined by

$$
D_{\mathrm{jet}} = \iint_{W_{A\,\mathrm{jet}}} [\rho u(U_\infty - u) + (P_\infty - P)]\,\mathrm{d}y\,\mathrm{d}z
$$

$$
D_{\mathrm{reg}} = \int\int_{S_2 - W_{A\,\mathrm{jet}}} [\rho u(U_\infty - u) + (P_\infty - P)]\,\mathrm{d}y\,\mathrm{d}z - \dot{m}U_\infty
$$

In the jet wake regions ($W_{A\,\mathrm{jet}}$), $U_\infty - u$ is negative (by definition); therefore, D_{jet} represents a thrust (a negative drag). Because our small perturbation method cannot be applied in the jet wake regions, we must evaluate the drag equation D_{jet} without applying the perturbation method. Rewriting equation D_{jet}, one can obtain

$$
\begin{aligned}
D_{\mathrm{jet}} &= \rho_\infty U_\infty^2 \iint_{W_{A\,\mathrm{jet}}} \frac{\rho}{\rho_\infty}\frac{u}{U_\infty}\left(1 - \frac{u}{U_\infty}\right)\mathrm{d}y\,\mathrm{d}z \\
&\quad + P_\infty \iint_{W_{A\,\mathrm{jet}}} \left(1 - \frac{P}{P_\infty}\right)\mathrm{d}y\,\mathrm{d}z
\end{aligned} \tag{46}
$$

Density ρ/ρ_∞ and pressure P/P_∞ can be calculated from Eqs. (11) and (12), respectively.

Assuming that u, T_T, and P_T are measured in the jet wake regions, the change in entropy $\Delta s/R$ can be evaluated from Eq. (38). Utilizing the definitions of the total temperature and speed of sound, $T_T = T[1 + (\gamma - 1)M^2/2]$ and $a^2 = \gamma RT$, T/T_∞ can be expressed as

$$\frac{T}{T_\infty} = \frac{T_T}{T_{T_\infty}}\left(1 + \frac{\gamma - 1}{2}M_\infty^2\right) - \frac{\gamma - 1}{2}M_\infty^2\left(\frac{u}{U_\infty}\right)^2 \tag{47}$$

Finally, substituting the values of ρ/ρ_∞ and P/P_∞ [calculated from Eqs. (11) and (12)] into Eq. (46), one can calculate the engine thrust D_{jet} (≤ 0).

In the regular wake region ($S_2 - W_{A\,\text{jet}}$) our small perturbation assumptions are valid, and all of the drag equations discussed in this paper are applicable. However, for the Maskell's induced drag calculation D_{Mi}, it is recommended to set the value of the vorticity ξ in the jet wake regions as, fictitiously, zero

$$\xi = \begin{cases} \xi : \text{regular wake } (S_2 - W_{A\,\text{jet}}) \\ 0 : \text{jet wake regions } (W_{A\,\text{jet}}) \end{cases} \tag{48}$$

Because of this treatment, the entire wake S_2 can now be handled as one regular wake, also nullifying the effect of jet wakes on Maskell's induced drag. Thus, the Poisson solvers discussed in the preceding section can still be used regardless of whether the model wake contains jet wakes or not.

Acknowledgments

We would like to thank N. J. Yu, J. D. McLean, G. D. Miller, and L. B. Wigton of Boeing Enabling Technology Research for many valuable discussions and comments over the course of developing the current method. We are especially grateful to L. B. Wigton for developing a new fast Poisson solver for our Maskell's induced drag analysis. Further thanks to D. H. Reed, who is the manager of the Acoustics and Fluid Mechanics group at Boeing, for his financial support and his encouragement, both of which paved the way for the completion of this project.

References

[1]Betz, A., "A Method for the Direct Determination of Profile Drag," *Zeitschrift für Flugtechnik und Motorluftschiffahrt*, Vol. 16, 1925, pp. 42–44 (in German).

[2]Maskell, E. C., "Progress Towards a Method for the Measurement of the Components of the Drag of a Wing of Finite Span," Royal Aircraft-Establishment, RAE TR 72232, London, Dec. 1972.

[3]Brune, G. W., "Quantitative Low-Speed Wake Surveys," *Journal of Aircraft*, Vol. 31, No. 2, 1994, pp. 249–255.

[4]Veldhuis, L. L. M., and Rentema, D. W. E., "Quantitative Wake Surveys Behind a Tractor Propeller-Wing Configuration," AIAA Paper 95-3908, Sept. 1995.

[5]Crowder, J. P., Watzlavick, R. L., and Krutckoff, T. K., "Airplane Flow-Field Measurements," Society of Automotive Engineers, Paper 975535, Oct. 1997.

[6]Kusunose, K., "Development of a Universal Wake Survey Data Analysis Code," AIAA Paper 97-2294, June 1997.

[7]Takahashi, T. T., "On the Decomposition of Drag from Wake Survey Measurements," AIAA Paper 97-0717, Jan. 1997.

[8]Van Dam, C. P., Nikfetrat, K., Wong, K, and Vijgen, P. M. H. W., "Drag Prediction at Subsonic and Transonic Speeds Using Euler Methods," *Journal of Aircraft*, Vol. 32, No. 4, 1995, pp. 839–845.

[9]Van Dam, C. P., "Recent Experience with Different Methods of Drag Prediction," *Progress in Aerospace Sciences*, Vol. 35, No. 8, 1999, pp. 751–798.

[10]Cummings, R. M., Giles, M. B., and Shrinivas, G. N., "Analysis of the Elements of Drag in Three-Dimensional Viscous and Inviscid Flows," AIAA Paper 96-2482, June 1996.

[11]Kusunose, K., "Drag Prediction Based on a Wake-Integral Method," AIAA Paper 98-2723, June 1998.

[12]Kusunose, K., Crowder, J. P., and Miller, G. D., "Installed Powered Engine Effects on Drag Using a Wake-Integral Method," AIAA Paper 2000-2400, June 2000.

[13]Kusunose, K., "Lift Analysis Based on a Wake-Integral Method," AIAA Paper 2001-0420, Jan. 2001.

[14]Cole, J. D., *Perturbation Methods in Applied Mathematics*, Blaisdell, Waltham, MA, 1968, pp. 1–78.

[15]Kusunose, K., Crowder, J. P., and Watzlavick, R. L., "Wave Drag Extraction from Profile Drag Based on a Wake-Integral Method," AIAA Paper 99-0275, Jan. 1999.

[16]Liepmann, H. W., and Roshko, A., *Elements of Gasdynamics*, Wiley, New York, 1956, pp. 17–20, 43–45.

[17]Shapiro, A. H., *The Dynamics and Thermodynamics of Compressible Fluid Flow*, Wiley, New York, 1953, pp. 41–43.

[18]Oswatitsch, K., *Gas Dynamics*, Academic Press, New York, 1956, pp. 209, 32–35.

[19]van der Vooren, J., and Slooff, J. W., "CFD-Based Drag Prediction; State-of-the-Art, Theory, Prospects," National Aerospace Lab., Technical Publ., TP 90247 U, Amsterdam, The Netherlands, Sept. 1992.

[20]Weston, R. P., "Refinement of a Method for Determining the Induced and Profile Drag of a Finite Wing from Detailed Wake," Ph.D. Dissertation, Dept. of Engineering Sciences, Univ. of Florida, Gainesville, March 1981.

[21]Kusunose, K., and Crowder, J. P., "Physical Properties of Maskell's Induced Drag Integral," AIAA Paper 2001-0421, Jan. 2001.